

Texture Development in (Nd,Ce)-Fe-B-type Die-upset Hybrid Magnet Consisted of Two Hard Magnetic Constituents

M. S. Kang¹, H. W. Kwon^{1*}, D. R. Djuanda², J. G. Lee³, and H. J. Kim⁴

¹*Pukyong National University, Busan 48513, Republic of Korea*

²*Metal Industries Development Center, Bandung 40135, Indonesia*

³*Korea Institute of Materials Science, Changwon 51508, Republic of Korea*

⁴*KITECH, Incheon 31056, Republic of Korea*

(Received 29 October 2019, Received in final form 17 December 2019, Accepted 17 December 2019)

Texture development in the Ce-substituted Nd-Fe-B-type die-upset hybrid magnet, which was fabricated using starting materials of Ce-substituted $(\text{Nd}_{0.55}\text{Ce}_{0.45})_{15}\text{Fe}_{72.2}\text{Co}_{6.6}\text{Ga}_{0.6}\text{B}_{5.6}$ HDDR-treated alloy powder and melt-spun $\text{Nd}_{13.6}\text{Fe}_{73.6}\text{Co}_{6.6}\text{Ga}_{0.6}\text{B}_{5.6}$ flakes (MQU-F) without Ce, was investigated. Noticeably better texture developed in die-upset magnet from the MQU-F flakes alone with respect to magnet from the HDDR-treated powder alone. Better texture developed also in the MQU-F flake regions in the die-upset hybrid magnet with respect to the HDDR particle regions, and overall texture in the hybrid magnet was dominantly controlled by the texture in the MQU-F flake regions. Overall texture in the hybrid magnet was not as good as the weighted average of texture expected from texture of the single alloy magnets from the HDDR powder alone and the MQU-F flakes alone.

Keywords : Nd-Fe-B magnet, Ce-substitution, die-upset magnet, texture, grain alignment

1. Introduction

Nd-Fe-B-type magnet has been making its big time in the high performance permanent magnet market, but there has been a chronic apprehension of limited supply and volatile price of raw materials of rare-earth metals. Regarding the supply risk of rare-earth for Nd-Fe-B-type magnet, what has recently emerged from permanent magnet community is so-called ‘rare-earth balanced magnet’ [1-3]. This claim advocates exploitation of abundant and cheap light rare-earths as coping strategy for supply risk of rare-earth metals and helps maintain balance between supply and demand of the rare-earth resources. The light rare earths such as La, Ce, Pr and Nd are mostly refined from rare-earth ores of Bastnasite and Monazite. Interestingly, the most abundant rare-earth element in those ores is cerium (Ce), and its supply in the market well outweighs its demand, thus Ce metal is available with much more affordable price than Nd and Pr [4, 5]. For substantiating the ‘rare-earth balanced magnet’, an extensive research

has been made to exploit Ce as a substituent for Nd and Pr in the (Nd,Pr)-Fe-B-type magnet [6-13]. Our previous report [14] revealed that hybrid magnet (die-upset) composed of two different types of Nd-Fe-B-type materials with and without Ce-substitution was feasible to be a good example of the ‘rare-earth balanced magnet’. In the die-upset hybrid magnet, texture, which decisively contributes to magnetic performance, was dependent upon the mixing ratio of the two constituent materials for hybridization. In the present study, we investigated in great detail texture development in the Ce-substituted Nd-Fe-B-type die-upset hybrid magnet.

2. Experimentals

Ce-substituted (Nd,Ce)-Fe-B-type hybrid magnet was fabricated by die-upset technique using mixture of two different types of Nd-Fe-B-type materials with and without Ce-substitution: Ce-substituted $(\text{Nd}_{0.55}\text{Ce}_{0.45})_{15}\text{Fe}_{72.2}\text{Co}_{6.6}\text{Ga}_{0.6}\text{B}_{5.6}$ HDDR-treated alloy powder and commercially available melt-spun $\text{Nd}_{13.6}\text{Fe}_{73.6}\text{Co}_{6.6}\text{Ga}_{0.6}\text{B}_{5.6}$ flakes (MQU-F) without Ce. The HDDR-treated alloy powders and MQU-F flakes were thoroughly mixed, and the mixture was first hot-pressed at 670 °C to obtain full density

©The Korean Magnetism Society. All rights reserved.

*Corresponding author: Tel: +82-51-629-6353

Fax: +82-51-629-6353, e-mail: hkwkwon@pknu.ac.kr

isotropic compact and then die-upset at 735 °C with 75 % thick reduction to render the compact anisotropic magnet having good texture. Overall texture developed in the hybrid magnet was evaluated by magnetic means: remanences measured along different directions parallel and perpendicular to pressing direction in die-upsetting were compared. Magnetic measurement was performed using a vibrating sample magnetometer (VSM) after magnetizing with 5 Tesla pulsing field. Microstructure of the sample were observed by a transmission electron microscope (TEM) and a scanning electron microscope (SEM).

3. Results and Discussion

Since whether $\text{Nd}_2\text{Fe}_{14}\text{B}$ -type grains in the starting materials have texture or not can influence texture development in the final hybrid magnet fabricated using them, examining texture in the starting materials is potentially needed in the first place for precise addressing of texture development in the hybrid magnet. Texture in the starting materials was examined by magnetic means. As-prepared HDDR and MQU-F particles were pulverized first to have near equi-axed shape so that demagnetizing factor of the particle is constant regardless of direction of its axis. If particle has irregular shape deviating from equi-axed shape it has different demagnetizing factor depending on direction of its axis. Then, despite having no grain texture, the irregular shaped particles could be somewhat aligned under applied field in a way that the direction with smallest demagnetizing factor is parallel to applied field. Evaluation of grain texture using irregular shaped particles like the as-prepared starting materials particles (Fig. 1(a), (c)) thus likely to twist into misleading conclusion about true nature of texture. The pulverized equi-axed particles were then aligned by applying magnetic field (1.5 T) and fixed with paraffin wax. Remanence values along parallel and perpendicular to the aligning direction were more or less identical, indicating surely that the starting HDDR-treated particle and the melt-spun flake were magnetically isotropic and not aligned. What was certain from this observation was that $\text{Nd}_2\text{Fe}_{14}\text{B}$ -type fine grains in the

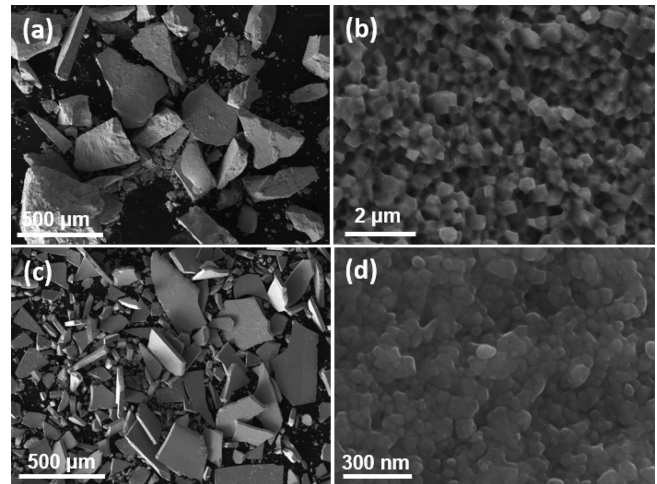


Fig. 1. Morphology of the as-prepared starting material particle and grain in it. (a) and (b) HDDR-treated $(\text{Nd}_{0.55}\text{Ce}_{0.45})_{15}\text{Fe}_{72.2}\text{Co}_{6.6}\text{Ga}_{0.6}\text{B}_{5.6}$ powder, (c) and (d) melt-spun $\text{Nd}_{13.6}\text{Fe}_{73.6}\text{Co}_{6.6}\text{Ga}_{0.6}\text{B}_{5.6}$ flake (MQU-F).

particle and flake have no grain texture: c-axis (EMD) of the fine $\text{Nd}_2\text{Fe}_{14}\text{B}$ -type phase grains orient randomly. Morphology and magnetic characteristics of the starting materials were shown in Fig. 1 and Table 1, respectively.

Texture developed in the hybrid magnet fabricated from a mixture of HDDR-treated powder and MQU-F flake with varying mixing ratio was evaluated by comparing demagnetization curves measured parallel and perpendicular to the pressing direction (Fig. 2). Among the magnetic performance parameters available from the demagnetization curve is remanence, which is most closely linked to texture developed in the die-upset magnet. For evaluation of texture in a permanent magnet, commonly adopted measure of texture is the degree of grain alignment (DoA), which was defined by comparing the remanence values measured parallel and perpendicular to the pressing direction: $\text{DoA} = ((M_{r(\parallel)} - M_{r(\perp)})/M_{r(\parallel)})$, where $M_{r(\parallel)}$ and $M_{r(\perp)}$ denote remanence values measured parallel and perpendicular to the pressing direction, respectively. Estimated DoA values for the hybrid die-upset magnets with varying mixing ratio were presented in Fig. 3. Also included

Table 1. Microstructural and magnetic properties of the starting materials of HDDR-treated alloy powder and melt-spun flakes for fabrication of hybrid magnet.

Starting materials	Composition	iHc (kOe)	Mr (kG)	$(\text{BH})_{\text{max}}$ (MGOe)	Average particle size (mm)	Average grain size (nm)	Aspect ratio of grain	Grain texture
HDDR-treated powder	$(\text{Nd}_{0.55}\text{Ce}_{0.45})_{15}\text{Fe}_{72.2}\text{Co}_{6.6}\text{Ga}_{0.6}\text{B}_{5.6}$	3	6.3	5.8	200	300-800	1.08	no
melt-spun flake (MQU-F)	$\text{Nd}_{13.6}\text{Fe}_{73.6}\text{Co}_{6.6}\text{Ga}_{0.6}\text{B}_{5.6}$	20	7.4	7.2	300	40-80	1	no

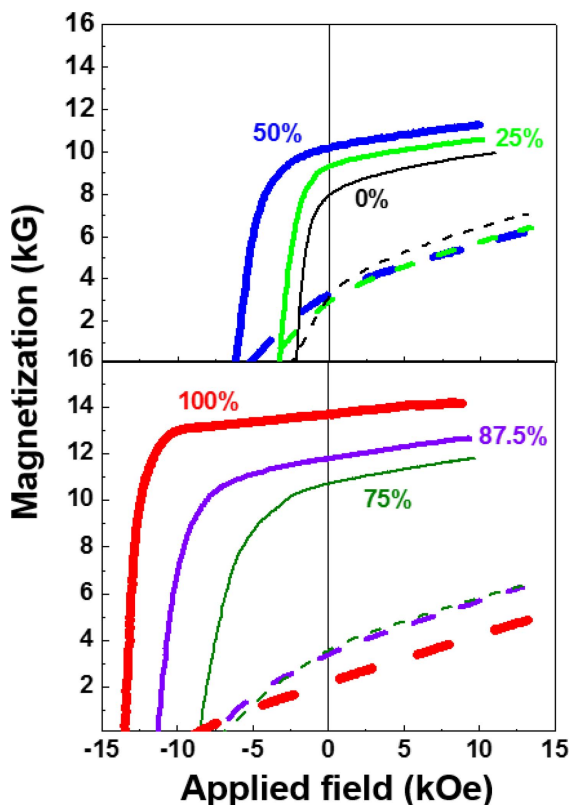


Fig. 2. (Color online) Demagnetisation curves of the hybrid magnets with varying MQU-F addition measured parallel and perpendicular to the pressing direction of die-upsetting.

in Fig. 3 were DoA values of the die-upset magnets from HDDR-treated powder and MQU-F flakes alone. It appeared that DoA of the magnet from HDDR-treated powder alone was markedly smaller than that of the magnet from MQU-F flakes alone. It was also noted that DoA value of the hybrid magnet added with MQU-F was noticeably higher with respect to the magnet from Ce-containing HDDR-treated powder alone. For better discussion of texture development in the hybrid magnets, full understanding of texture formation mechanism operating in the Nd-Fe-B-type die-upset magnet is potentially needed. Texture in the Nd-Fe-B-type die-upset magnet is generally known to develop by mechanism of dissolution, precipitation and grain rotation via grain boundary gliding [15, 16]. Nd-Fe-B-type alloy for a die-upset magnet has slightly over-stoichiometric composition, thus being consisted mostly of $\text{Nd}_2\text{Fe}_{14}\text{B}$ -type matrix magnetic phase and Nd-rich grain boundary phase. During die-upsetting the $\text{Nd}_2\text{Fe}_{14}\text{B}$ -type phase exists as solid, whereas the Nd-rich grain boundary phase becomes liquid. Most importantly, the tetragonal $\text{Nd}_2\text{Fe}_{14}\text{B}$ -type phase crystal, which will exhibit *c*-axis (easy magnetization direction: EMD) texture along pressing direction during die-upsetting, has anisotropy

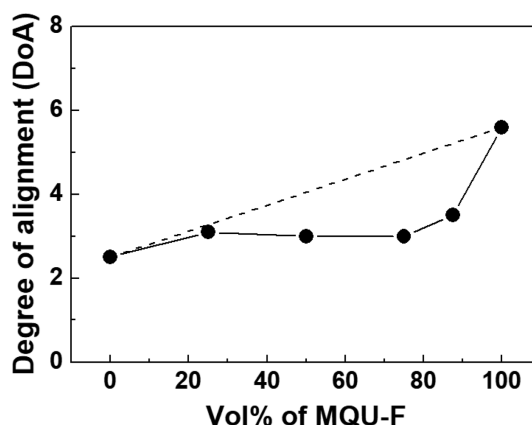


Fig. 3. (Color online) Variations of DoA in the hybrid magnet and aspect ratio of grains in each constituent region in the hybrid magnet with varying MQU-F addition.

in mechanical properties: elastic modulus of the crystal along *c*-axis is considerably lower than that along *a*-axis (hard magnetization direction: HMD) [17]. $\text{Nd}_2\text{Fe}_{14}\text{B}$ -type grains in the hot-pressed compact have no texture and orient randomly (Fig. 4(a)), and some of the grains (favorable grains) that have their *c*-axis accidentally parallel with pressing direction of die-upsetting are placed in a state of lower strain energy due to the anisotropy of elastic modulus. While the grains (unfavorable grains) with *c*-axis out of pressing direction are in a state of higher strain energy. Thus, atoms in the unfavorable grains resultantly become less stable under pressure. As a result, the unfavorable grains are more likely to dissolve and the dissolved atoms move into liquid Nd-rich grain boundary phase. The dissolved atoms in the liquid grain boundary phase are now tending to precipitate preferentially onto the surface of undissolved favorable grains that are in more stable state in terms of strain energy. Most importantly, the location where the dissolved atoms preferentially precipitate on the surface of undissolved favorable grains is closely linked with texture development. Thanks to anisotropic mechanical properties of the $\text{Nd}_2\text{Fe}_{14}\text{B}$ -type phase crystal again, the top and bottom surfaces of the favorable grains are under higher strain energy state, whereas the lateral surface is in lower strain energy state under pressure during die-upsetting. The dissolved atoms in the liquid grain boundary phase, thus, tend to preferentially precipitate on the lateral surface rather than on top and bottom surfaces of the undissolved favorable grains, rendering the equi-axed favorable grains into platelet (pancake) shape (Fig. 4(b), (c)). Thanks to their plate-like geometry, the favorable $\text{Nd}_2\text{Fe}_{14}\text{B}$ -type grains with their *c*-axis being perpendicular to wide plane will be further aligned better in the course of deformation via

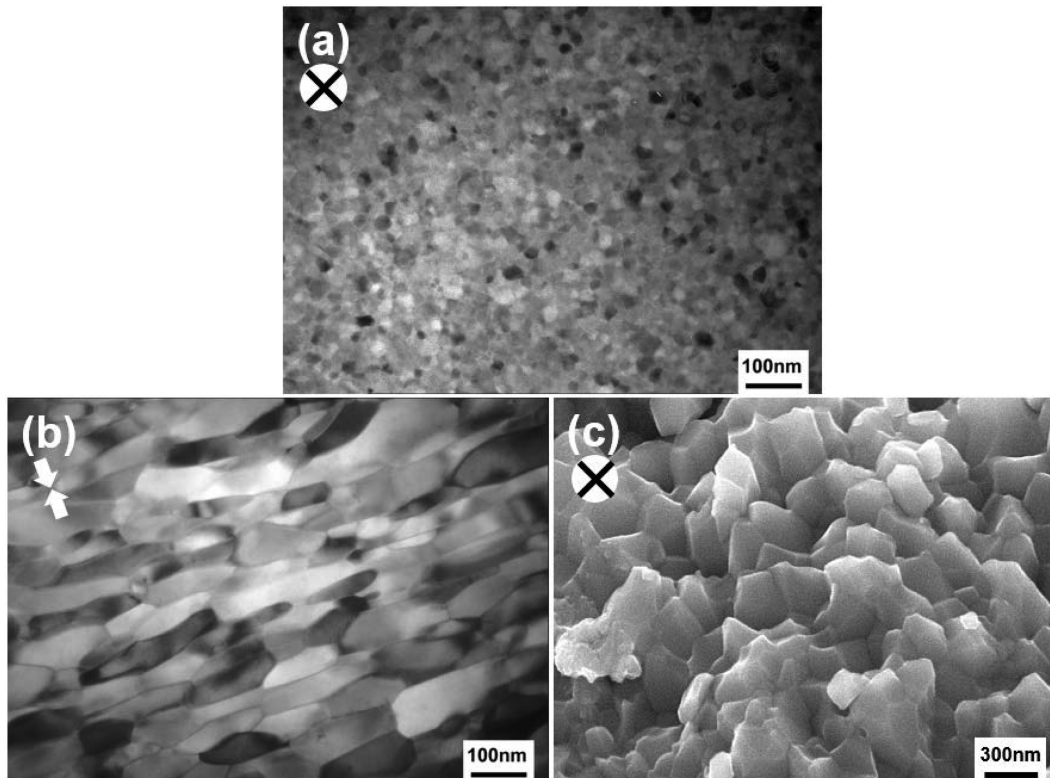


Fig. 4. (a) TEM photo showing microstructure and grain morphology in hot-pressed compact of melt-spun $\text{Nd}_{13.6}\text{Fe}_{73.6}\text{Co}_{6.6}\text{Ga}_{0.6}\text{B}_{5.6}$ flake (MQU-F). TEM and SEM photos showing grain morphology observed on the plane (b) parallel and (c) perpendicular to pressing direction respectively in the die-upset magnet from the hot-pressed compact. (arrows indicate pressing direction)

grain boundary gliding, thus leading to good texture. Smaller DoA value (less texture) for the die-upset magnets from HDDR-treated powder alone with respect to the magnet from MQU-F flakes alone can now be fully understood by considering this texture formation mechanism. Due to larger grain size (Fig. 1 and Table 1), unfavorable grains in the HDDR-treated powder cannot be completely dissolved during the quick die-upsetting, and many unfavorable grains may still remain. On top of that, limited precipitation of the dissolved atoms on the lateral surface of larger favorable grain may lead to immature plate-like shape because of larger grain size. Under this circumstance, less profound texture may develop in the course of die-upsetting. On the contrary, since grain size of the MQU-F flakes is considerably finer (Fig. 1 and Table 1), it is more likely that the unfavorable grains may dissolve completely and disappear in the die-upset magnet prepared from MQU-F flakes alone. On top of that, profuse precipitation of the dissolved atoms on the lateral surface of finer favorable grains may lead to more mature plate-like shape because of smaller grain size. Thus, more profound texture may develop in the course of die-upsetting. Texture developed in the hybrid magnet can also be evaluated by observing grain morphology. As can be readily understood from

the texture formation mechanism, grains in the magnet with better texture may have better developed plate-like shape, that is to say, larger aspect ratio (diameter/thickness of platelet grain). As can be seen in Fig. 5, grains in the die-upset magnet from MQU-F alone have remarkably larger aspect ratio (more elongated appearance) with respect to the die-upset magnet from HDDR powder alone. Better texture development in die-upset magnet from MQU-F with respect to magnet from HDDR powder was reported previously [18-21]. In the die-upset hybrid magnet, better texture is also believed to develop in MQU-F flake regions with respect to HDDR particle regions and this is evidenced by markedly greater aspect ratio of grains in MQU-F region with respect to HDDR particle region (Fig. 5). Since overwhelmingly better texture is developed in MQU-F flake regions in the die-upset hybrid magnet, overall texture in the hybrid magnet is probably controlled dominantly by the texture in MQU-F regions.

What caught our attention in connection with texture development in the hybrid die-upset magnet is that DoA of hybrid magnet was lower with respect to the weighted average DoA value estimated from DoA of single alloy magnets from HDDR powder alone and MQU-F flakes alone. If we assume that DoA in each constituent part in

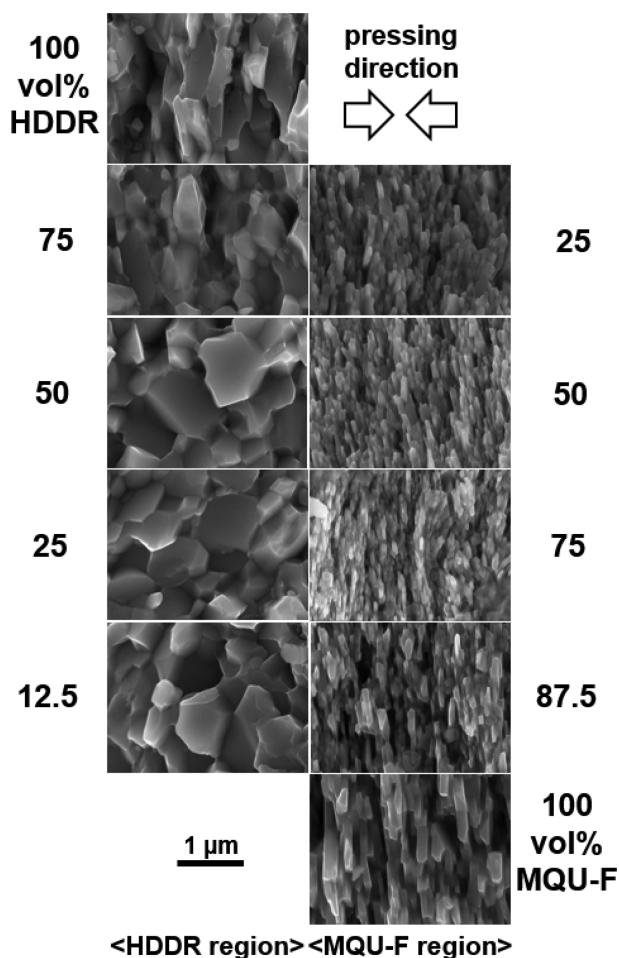


Fig. 5. SEM photos showing morphology of grains in the HDDR particle and MQU-F flake regions in the hybrid magnet with varying MQU-F addition.

the hybrid magnet would be same as what would develop in the die-upset magnets prepared from HDDR powder and MQU-F flakes alone, overall texture of the hybrid magnet would, then, be given according to a mixture law (weighted average): Overall DoA of the hybrid magnet would lie at the corresponding value on the straight dotted line connecting the DoA values for the die-upset magnets from HDDR-treated powder and from MQU-F flakes alone (Fig. 3). As can be seen, measured overall texture of the hybrid magnet, however, appears to be measurably lower with respect to value expected from the mixture law. This indicates that texture in each constituent region in the hybrid magnet has been less developed with respect to that developed in the die-upset magnet from HDDR-treated powder and from MQU-F flakes alone. Less developed texture in each constituent region in the hybrid magnet can be understood again by considering the texture formation mechanism. When hot-pressed compact of the mixture of HDDR powder and MQU-F flakes was press-

ed during die-upsetting, the stress exerting on MQU-F part, which dominantly controlled overall texture of the hybrid magnet, may be somewhat lessened compared to the case with MQU-F flakes alone. In accordance with the Hall-Petch relation [22-24], which states dependency of mechanical strength of polycrystalline metal alloys on the grain size, the HDDR-treated particle part with larger grain structure may have lower flow stress during plastic deformation by die-upsetting with respect to the MQU-F flake part with much finer grain structures. Under pressure for die-upsetting, the HDDR-treated particle part having lower flow stress is easily deformed first and squeezed out, acting like stress-absorbing layers. Under this circumstance, the stress practically exerting on MQU-F part is somewhat lessened compared to the case of single alloy magnet with MQU-F flakes alone. Then, as expected from the texture formation mechanism, texture may develop less actively in the MQU-F part in the hybrid magnet, which dominantly controls overall texture, leading to less profound overall texture.

4. Conclusion

Noticeably better texture developed in the die-upset magnet from the MQU-F flakes alone with respect to magnet from the HDDR-treated powder alone. Better texture developed also in the MQU-F flake region in the die-upset hybrid magnet with respect to the HDDR particle region, and overall texture in the hybrid magnet was dominantly controlled by the texture in MQU-F flake regions. Overall texture in the hybrid magnet was not as good as the weighted average of texture expected from texture of the single alloy magnets from the HDDR powder alone and the MQU-F flakes alone.

Acknowledgement

The authors gratefully acknowledge that the present work was financially supported by the Technology Innovation Program from the Ministry of Trade, Industry & Energy (MOTIE, Republic of Korea) (No. 10080382).

References

- [1] P. Falconnet, *J. Less-Common Met.* **111**, 9 (1985).
- [2] K. Binnemans, P. T. Jones, K. Van Acker, B. Blanpain, B. Mishra, and D. Apelian, *J. Magn.* **65**, 846 (2013).
- [3] O. Gutfleisch, M. A. Willard, E. Bruck, C. H. Chen, S. G. Sankar, and J. P. Liu, *Adv. Mater.* **23**, 821 (2011).
- [4] P. Falconnet, *Proceedings of: First Workshop on the Basic and Applied Aspects of Rare Earths* (Venice, Italy,

- 26-27th May, 1988), 19 (1989).
- [5] T. G. Goonan, U.S. Geological Survey Scientific Investigations Report 2011-5094, 15 (2011).
- [6] J. F. Herbst, M. S. Meyer, and F. E. Pinkerton, *J. Appl. Phys.* **111**, 07A718 (2012).
- [7] E. J. Skoug, M. S. Meyer, F. E. Pinkerton, M. M. Tessema, D. Haddad, and J. F. Herbst, *J. Alloys Compd.* **574**, 552 (2013).
- [8] A. Alam, M. Khan, R. W. Mccallum, and D. D. Johnson, *Appl. Phys. Lett.* **102**, 42402 (2013).
- [9] C. Yan, S. Guo, R. Chen, D. Lee, and A. Yan, *IEEE Trans. Magn.* **50**, 2102605 (2014).
- [10] A. K. Pathak, M. Khan, K. A. Gschneidner, Jr., R. W. Mccallum, L. Zhou, K. Sun, K. W. Dennis, C. Zhou, F. E. Pinkerton, M. J. Kramer, and V. K. Pecharsky, *Adv. Mater.* **27**, 2663 (2015).
- [11] Z. B. Li, B. G. Shen, M. Zhang, F. X. Hu, and J. R. Sun, *J. Alloys Compounds* **628**, 325 (2015).
- [12] A. K. Pathak, M. Khan, K. A. Gschneidner, Jr., R. W. Mccallum, L. Zhou, K. Sun, and M. J. Kramer, *Acta Mater.* **103**, 211 (2016).
- [13] Z. B. Li, M. Zhang, B. G. Shen, F. X. Hu, and J. R. Sun, *Mater. Lett.* **172**, 102 (2016).
- [14] Dagus R. Djuanda, M. S. Kang, H. W. Kwon, J. G. Lee, and H. J. Kim, *J. Magn.* (2019), in press.
- [15] L. Li and C. D. Graham, Jr., *J. Appl. Phys.* **67**, 4756 (1990).
- [16] L. Li and C. D. Graham, Jr., *IEEE Trans. Magn.* **28**, 2130 (1992).
- [17] Y. Luo and N. Zhang, 10th International Workshop on Rare-Earth Magnets and Their Applications, Kyoto, Japan. 275 (1989).
- [18] A. Kirchner, W. Grunberger, O. Gutfleisch, V. Neu, K. H. Muller, and L. Schultz, *J. Phys. D, Appl. Phys.* **31**, 1660 (1998).
- [19] S. Liesert, A. Kirchner, W. Grunberger, A. Handstein, P. De Rango D. Fruchart, L. Schultz, and K.-H Muller, *J. Alloys Compounds* **266**, 260 (1998).
- [20] P. J. McGuinness, C. Short, A. F. Wilson, and I. R. Harris, *J. Alloys Compounds* **184**, 243 (1992).
- [21] H. R. Cha, J. G. Yoo, K. W. Jeon, Y. K. Baek, H. W. Kwon, D. Lee, and J. G. Lee, *IEEE Trans. Magn.* **53**, 2101204 (2017).
- [22] E. O. Hall, *Proc. Phys. Soc. B* **64**, 747 (1951).
- [23] N. J. Petch, *J. Iron Steel Inst.* **174**, 25 (1953).
- [24] J. G. Sevillano, P. Van Houtte, and E. Aernoudt, *Prog. Mater. Sci.* **25**, 69 (1981).